

# Translating Clinical Delineation of Diabetic Foot Ulcers into Machine Interpretable Segmentation

Connah Kendrick, Bill Cassidy, Joseph M. Pappachan, Claire O'Shea, Cornelious J. Fernandez, Elias Chacko, Koshy Jacob, Neil D. Reeves, and Moi Hoon Yap, *Senior Member, IEEE*

**Abstract**—Diabetic foot ulcer is a severe condition that requires close monitoring and management. For training machine learning methods to auto-delineate the ulcer, clinical staff must provide ground truth annotations. In this paper, we propose a new diabetic foot ulcers dataset, namely DFUC2022, the largest segmentation dataset where ulcer regions were manually delineated by clinicians. We assess whether the clinical delineations are machine interpretable by deep learning networks or if image processing refined contour should be used. By providing benchmark results using a selection of popular deep learning algorithms, we draw new insights into the limitations of DFU wound delineation and report on the associated issues. This paper provides some observations on baseline models to facilitate DFUC2022 Challenge in conjunction with MICCAI 2022. The leaderboard will be ranked by Dice score, where the best FCN-based method is 0.5708 and DeepLabv3+ achieved the best score of 0.6277. This paper demonstrates that image processing using refined contour as ground truth can provide better agreement with machine predicted results. DFUC2022 will be released on the 27th April 2022.

**Index Terms**—Clinical delineation, deep learning, DFUC2022, diabetic foot ulcers, segmentation

## I. INTRODUCTION

Diabetic Foot Ulcers (DFU) are caused when sections of the foot and skin are damaged due to multiple factors including nerve damage (diabetic peripheral neuropathy) and foot deformities. DFU healing can be impaired due to blood flow (vascular) limitations as a consequence of diabetes. Owing to this, the DFU requires regular checks to ensure optimal healing and to inform any adjustments to the treatment strategy. DFU frequently become infected and can lead to amputation and in some cases loss of life if the antibiotic treatment is unsuccessful [1]. It is shown that at least 10% of people with diabetes will have some form of DFU in their lifetime, rising

Date submitted for review: 21 April 2022. We gratefully acknowledge the support of NVIDIA Corporation who provided access to GPU resources and sponsored Diabetic Foot Ulcers Grand Challenges.

C. Kendrick, B. Cassidy and M.H. Yap are with the Department of Computing and Mathematics, Manchester Metropolitan University (e-mail: Connah.Kendrick@mmu.ac.uk, M.Yap@mmu.ac.uk).

J. Pappachan is with the Lancashire Teaching Hospitals NHS Foundation Trust (e-mail: pappachan.joseph@lthtr.nhs.uk).

C. O'Shea is with Waikato District Health Board (e-mail: claire.o'shea@waikatodhb.health.nz).

C. J. Fernandez is with United Lincolnshire Hospitals NHS Trust (e-mail: drcjfernandez@yahoo.com).

E. Chacko is with Jersey General Hospital (e-mail: e.chacko@health.gov.je).

K. Jacob is with Eastbourne District General Hospital (e-mail: drkoshyjacob@gmail.com).

N. D. Reeves is with the Research Centre for Musculoskeletal Science & Sports Medicine (e-mail: n.reeves@mmu.ac.uk).

to 25% depending on life-style factors [2], [3]. Moreover, recent studies have shown that after treatment, patients have a 70% chance of ulcer recurrence [4]. Although DFU is a physical disease, it has also been widely reported to have a drastic impact on patient mental well-being and quality of life, causing anxiety and depression [5].

Treatment for DFU can be a long term process, due to diabetes-related complications impairing the healing process [6]. It requires a multi-disciplinary team [7] to monitor the progress of the ulcer, focusing largely on the management of diabetes [8] and blood flow to the foot. However, complications, such as infection [9] significantly prolong treatment. If treatment is prolonged, the possibility of infection and amputation increase significantly [10]. This has been shown to create a heavy burden on healthcare systems, in terms of both time and cost per patient [11], [7]. Furthermore, this causes a great deal of concern due to the predicted rapid global rise of diabetes [12], amplified significantly by the current pandemic [13]. To address these challenges, researchers have been working towards development of automated systems capable of detecting and monitoring DFU [14]. Improvements to automated delineation of DFU could support improved digital healthcare tools that could be used for screening and triage of DFU. Furthermore, these improvements could aid in the development of active DFU monitoring systems, to engage the healing process stage.

This paper demonstrates the processes of translating clinical delineation of DFU into machine interpretable segmentation. We contribute to the research progress of DFU segmentation in the following ways:

- Introduce the largest DFU segmentation dataset with ground truth delineation (namely, DFUC2022) and perform detailed analysis. DFUC2022 will be made available for research purposes and for the upcoming DFU Grand Challenge 2022 [15], in conjunction with MICCAI 2022.
- Investigate the effect of image processing refined contours on the performance of a popular deep learning segmentation algorithm, DeepLabv3+.
- Establish baseline results for the DFUC2022 dataset using a range of popular deep learning segmentation networks.

This work will benefit the research community by providing a summary of available datasets to access and use for training segmentation based networks. With our established partnerships between clinicians and researchers, we provide the largest DFU segmentation dataset with superior image resolution when compared with existing DFU datasets [18].

TABLE I  
A COMPARISON OF THE PROPOSED DFUC2022 DATASETS AND THE EXISTING DFU IMAGE SEGMENTATION DATASETS.

Publication	Year	Dataset Name	Resolution	Train	Test	Total
Wang et al. [16]	2020	AZH wound care dataset	$224 \times 224$	831	278	1,109
Thomas [17]	NA	Medetec	$560 \times 391$ $224 \times 224$	152	8	160
Wang et al. [18]	2021	FUSeg Challenge	$512 \times 512$	1010	200	1210
Proposed	2022	DFUC2022	$640 \times 480$	2000	2000	4000

Additionally, we provide an in-depth analysis on the performance of baseline results. To assist in fair assessment and comparison with the benchmarks, we release a testing set that can be evaluated online via a grand challenge website (<https://dfuc2022.grand-challenge.org/>), providing almost instant evaluation results on a standard set of performance metrics.

## II. RELATED WORK

The development of computer algorithms for DFU research was accelerated by data sharing, including the DFUC2020 dataset [19], the DFUC2021 dataset [20] and the Foot Ulcer Segmentation dataset [18]. This section summarises the publicly available segmentation datasets, for complete DFU datasets (including other tasks, such as ulcer detection and classification), we refer the reader to an overview of the DFU datasets development by Yap et al. [21]. Table I compares the existing DFU segmentation datasets to our proposed DFUC2022 dataset. It is noted that our dataset is the largest dataset (4000 images), with improved resolution and the inclusion of none-cropped images.

The first works in DFU segmentation using fully convolutional techniques were completed by Goyal et al. [22]. They performed segmentation experiments using a small dataset comprising 705 images with an FCN-16s network. They used 5-fold cross-validation with two-tier transfer learning resulting in a Dice Similarity Coefficient of 0.794 ( $\pm 0.104$ ) for segmentation of DFU region. These results were promising, however, the small size of the dataset is likely to impact the model’s ability to generalise in real-world use.

More recently, Wang et al. [23] conducted the Foot Ulcer Segmentation Challenge. This work focused on the development of segmentation CNNs using 1210 foot photographs exhibiting DFU which were collected over a 2 year period from 889 patients. They provided ground truth masks provided by wound care experts. However, many of the images were heavily padded to standardise image dimensions for training purposes. Additionally, although the images were shared as lossless PNG files, they exhibited notable compression artefacts, indicating that the original images had been heavily compressed before being converted to PNG. The provided ground truth files also appeared to be a mix of human and machine-generated masks. The winning team in the challenge, Mahbod et al. [24], used an ensemble of LinkNet and U-Net networks. They achieved a Dice Similarity Coefficient of 0.888. They used pretrained weights (EfficientNetB1 for

LinkNet and EfficientNetB2 for U-Net) with additional pre-training using the Medetec dataset. The challenge concluded that segmentation of small isolated areas of the wound with ambiguous boundaries were the most challenging aspects of the task. Conversely, segmentation of relatively larger wound regions showing clear boundaries where wound beds were cleansed, removing dead tissue, provided superior results. Cases clearly exhibiting infection, slough, or other impediments were also shown to provide improved results.

Current works in DFU segmentation show promising results. However, there are notable limitations to the datasets that were used to train these models. Aspects such as the quality and number of images may present issues that would negatively affect real-world application.

## III. DFUC2022 DATASETS

We have received approval from the UK National Health Service Research Ethics Committee (reference number is 15/NW/0539) to use diabetic foot ulcer (DFU) images for the purpose of this research. This paper introduces the largest DFU segmentation dataset, which consists of a training set of 2000 images and a testing set of 2000 images. The ulcer regions on these images were delineated by experienced podiatrists and consultants. We then preprocess the raw masks with an active contour algorithm [25]. Figure 1 illustrates an example of a DFU image showing a preprocessed region with active contour together with the expert delineation. Note that the boundary of the region is smoother after the preprocessing stage. To ensure that this smoothing process does not alter the clinical delineation, we report the agreement between expert delineation and refined contours, which produced a high agreement rate with a Dice Score of  $0.9650 \pm 0.0226$  and Mean Intersection Over Union (mIoU) of  $0.9332 \pm 0.0408$ . These metrics demonstrate that preprocessing did not significantly alter clinical delineation, where the number of DFUs are equivalent before and after preprocessing.

The DFUC2022 training set consists of 2304 ulcers, where the smallest ulcer size is 0.04% of the total image size, and the largest ulcer size is 35.04% of the total image size. Figure 2 provides an overview of the ratio of the delineated ulcer region to the total image size, where 89% (2054 out of 2304) of the ulcers are less than 5% of the total image size. The smaller images in particular represent a significant challenge for segmentation algorithms as it is widely known that deep learning algorithms have a tendency to miss small regions [26]. Another advantage of our dataset is that of the 2,000 training

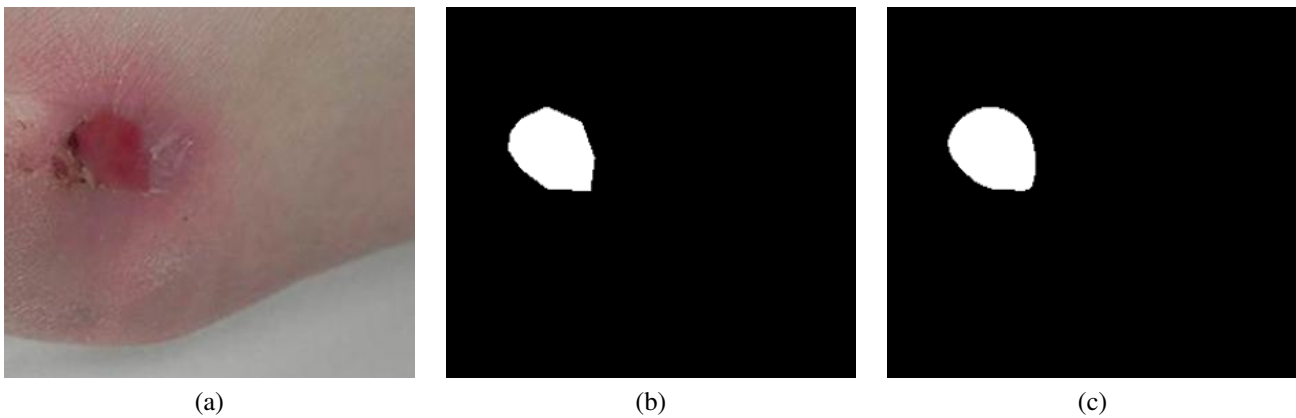


Fig. 1. Illustration of (a) an early onset DFU; (b) expert delineation; and (c) refined active contour shape.

images, there are 2,304 ulcers with an average of 1.152 ulcers per image.

To increase the level of challenge, we include a small number of duplicates, which were annotated by different experts. The duplicate examples demonstrate wound delineation where clinicians did not agree. Challenge participants will be able use the training set with or without further data curation, but re-annotation is not permitted by the challenge rules. In the test cases we provide a small sample of healthy / remission cases to test the reliability of trained networks against false positive results. Furthermore, some masks may contain artifacts (such as blur) from the resizing process.

#### IV. METHODS

This section describes the methods used to investigate the effect of image processing refined contours, summarises a range of popular baseline methods for medical image segmentation and a new strategy to improve the performance of the best segmentation method on the DFUC2022 dataset. We provide segmentation masks for the training set only, and use the grand-challenge website to allow participants to test their methods on an exclusive testing set. We provide a total of 4,000 images with 2,000 binary masks for training. The masks are coded 0 for background and 1 for the DFU region.

##### A. Manual delineation vs refined contours

While deep learning has gained popularity in biomedical image segmentation, there are unanswered questions concerning ground truth annotation, such as: (1) Would deep learning algorithms learn better with expert manual delineations (polygonal outlines) or image processing refined contours; and (2) which contour should be used for machine learning algorithms? To answer these questions in the context of DFUC2022, we run experiments with Deeplabv3+ [27], one of the popular deep learning algorithms for medical imaging research [28], [29]. Our intention is not to produce the best result, but to study the effect of coarse and detailed delineation on deep learning algorithms. Therefore, we select this algorithm without bias. First, we train two models using the default setting of Deeplabv3+, one on expert delineation and another on refined contour. We split the 2000 training images

into 1,800 images as training set and 200 images as validation set. Then, we test each model on the 2000 test set by using both expert delineation and refined contour as ground truth.

##### B. Baseline methods

We implement a wide range of existing deep learning segmentation models for the DFUC2022 baseline. These models cover a range of segmentation architectures, namely FCN [30], U-Net [31] and SegNet [32] with varying back-bones to process the data, such as VGG [33] and ResNet50 [34]. We also include a comparison of alternative network depths. The range of model diversity aims to provide a good indication of techniques suitable for DFU segmentation. These new insights can direct future works with a baseline to compare against and reduce the need for repeat training of these networks. In addition to the standard U-Net, SegNet models, we provide baselines for FCN8, FCN32, U-Net and SegNet with ResNet50 and VGG as backbones.

For training the baseline networks, we use all 2,000 training images, with 200 separate images for validation. We train the networks with the AdaDelta optimizer and a suggested learning rate of 0.001, decay of 0.95 and a stabilisation epsilon of  $1e - 07$ , using categorical cross-entropy loss. We train on multiple batch sizes (2, 32, and 96) and report the best result. We do not perform augmentation during training or post-processing on the final prediction masks, as our aim is to produce baselines and understanding of the DFUC2022 dataset. We train the networks until the validation accuracy fails to improve, with a patience of 10 epochs.

##### C. Performance metrics

In image segmentation, the commonly use evaluation metrics are:

Dice Similarity Index (Dice) as shown in Equation (1):

$$Dice = 2 * \frac{|X \cap Y|}{|X| + |Y| - |X \cap Y|} \quad (1)$$

and Intersection Over Union (IoU) (also known as Jaccard Index) as shown in Equation (2):

$$IoU = \frac{|X \cap Y|}{|X| + |Y|} \quad (2)$$

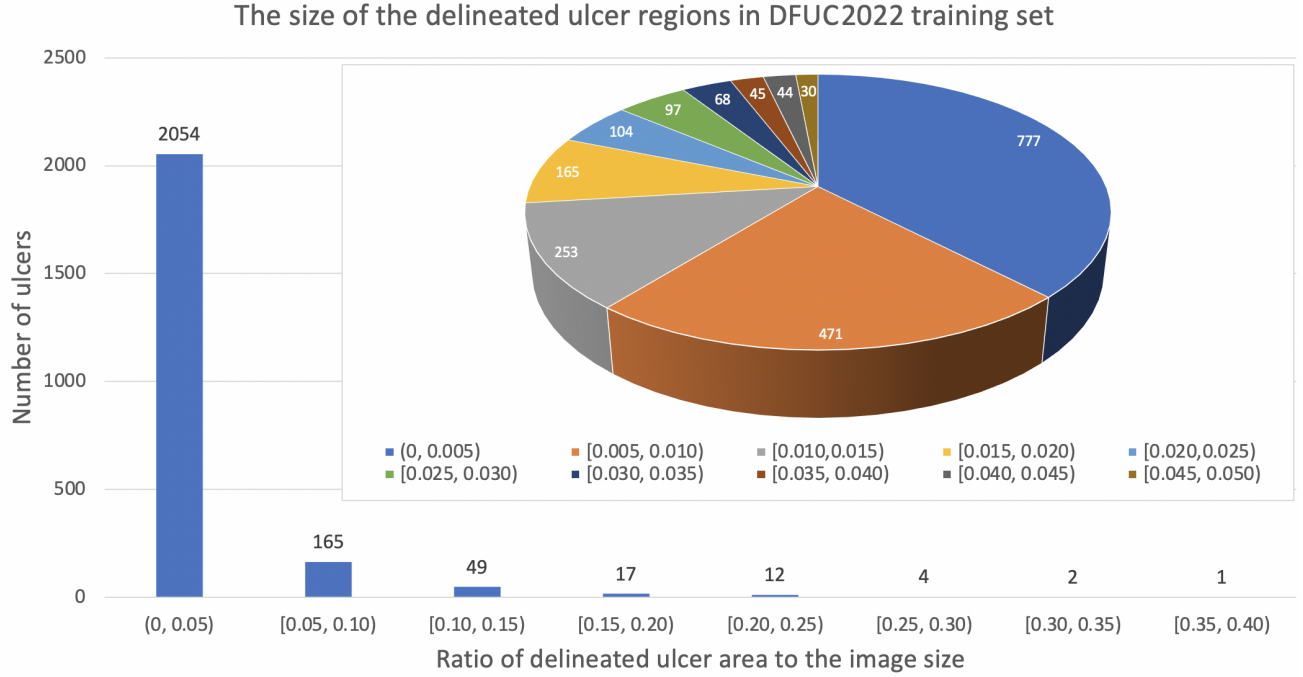


Fig. 2. The size of delineated ulcer regions in the DFUC2022 training set.

TABLE II  
COMPARISON OF THE RESULTS WHEN TRAINING WITH MANUAL DELINEATION AS GROUND TRUTH VS IMAGE PROCESSING REFINED CONTOUR AS GROUND TRUTH. THE RESULTS SHOW THE MACHINE PREDICTED MASKS HAVE BETTER AGREEMENT WITH THE REFINED CONTOUR.

Train	Test	Metrics	
		Dice	mIoU
Manual delineation	Manual delineation	0.5870±0.3135	0.4809±0.2993
Manual delineation	Refined contour	0.5930±0.3131	0.4871±0.2999
Refined contour	Manual delineation	0.6219±0.0286	0.5162±0.2967
Refined contour	Refined contour	<b>0.6277±0.3051</b>	<b>0.5224±0.2967</b>

where  $X$  and  $Y$  represent the ground truth mask and the predicted mask. We used mIoU to better represent the segmentation outcomes for both classes (ulcer and background).

For the DFUC2022 Challenge, we include additional metrics to help the participants to understand Type I and Type II errors, we evaluate the performance with two additional metrics:

False Positive Error (FPE) as in Equation (3):

$$FPE = \frac{FP}{FP + TN} \quad (3)$$

and False Negative Error (FNE) as in Equation (4).

$$FNE = \frac{FN}{FN + TP} \quad (4)$$

where  $FP$  is the total number of false positives in the predictions,  $TN$  is the total number of true negatives and  $FN$  is the total number of false negatives.

## V. RESULTS AND DISCUSSION

Table II shows the results when trained on two types of annotation: manual delineations vs refined contours. The

results show that the algorithm did not learn from the human delineation on the boundary (polygonal outlines). The refined contour consistently demonstrated closer agreement with the machine predictions, without relying on the type of ground truth used for training. Therefore, we use image processing refined contour as ground truth for both train set and test set, for the rest of the paper and the challenge.

As shown in Table III, many of the available techniques give reasonable results in DFU segmentation. Among the baseline methods, the best performing model was FCN32 with a VGG backbone, with the highest DICE score of 0.5708 and 0.4549 for mIoU. A key factor in this challenge is the network capabilities of handling images without positive DFU cases (True Negatives) thus we use the FPE metric. In such cases the best performing model is also FCN32 VGG, which shows a high understanding of the surround regions. We observe that most methods that use a higher batch size resulted in significant performance degradation. A contributing factor to this is likely to be background noise present in the images where the environment can vary significantly between images. Lower batch sizes allowed the system to focus on a case by case basis, allowing the network to slowly learn to ignore the

TABLE III

A COMPARISON OF THE OVERALL PERFORMANCE OF THE STATE-OF-THE-ART METHODS, RESULTS REPORTED ON THEIR BEST EPOCH. † = HIGHER SCORE IS BETTER; ⊖ = LOWER SCORE IS BETTER. WE TRAIN UNIQUE 12 MODELS, UNDER DIFFERENT BATCH SIZES. HOWEVER, WE ONLY SHOW THE MODELS WITH THE SETTINGS THAT RESULTED IN THE BEST PERFORMANCE. *Italic* INDICATES THE BEST BASELINE RESULT AND **BOLD** INDICATES THE BEST OVERALL RESULT.

Model	Backbone	Settings Best Batch Size	Metrics			
			Dice †	mIoU †	FPE ⊖	FNE ⊖
FCN8		2	0.2621	0.1914	0.6789	0.6062
	ResNet50	2	0.4993	0.3963	0.4576	<i>0.3824</i>
	VGG	2	0.5101	0.3952	0.3643	0.4500
FCN32		2	0.2174	0.1594	0.7564	0.6980
	ResNet50	2	0.4334	0.3372	0.5090	0.5081
	VGG	2	<i>0.5708</i>	<i>0.4549</i>	0.3396	0.3833
SegNet		32	0.2677	0.1880	0.6325	0.6510
	ResNet50	32	0.4768	0.3676	0.4325	0.4339
	VGG	32	0.4596	0.3469	0.4003	0.5158
U-Net		2	0.4057	0.3035	0.4900	0.5119
	ResNet50	32	0.0646	0.0371	0.5585	0.9584
	VGG	2	0.1446	0.0878	<i>0.2501</i>	0.9020
DeepLabv3+		2	<b>0.6277</b>	<b>0.5224</b>	<b>0.3266</b>	<b>0.2859</b>

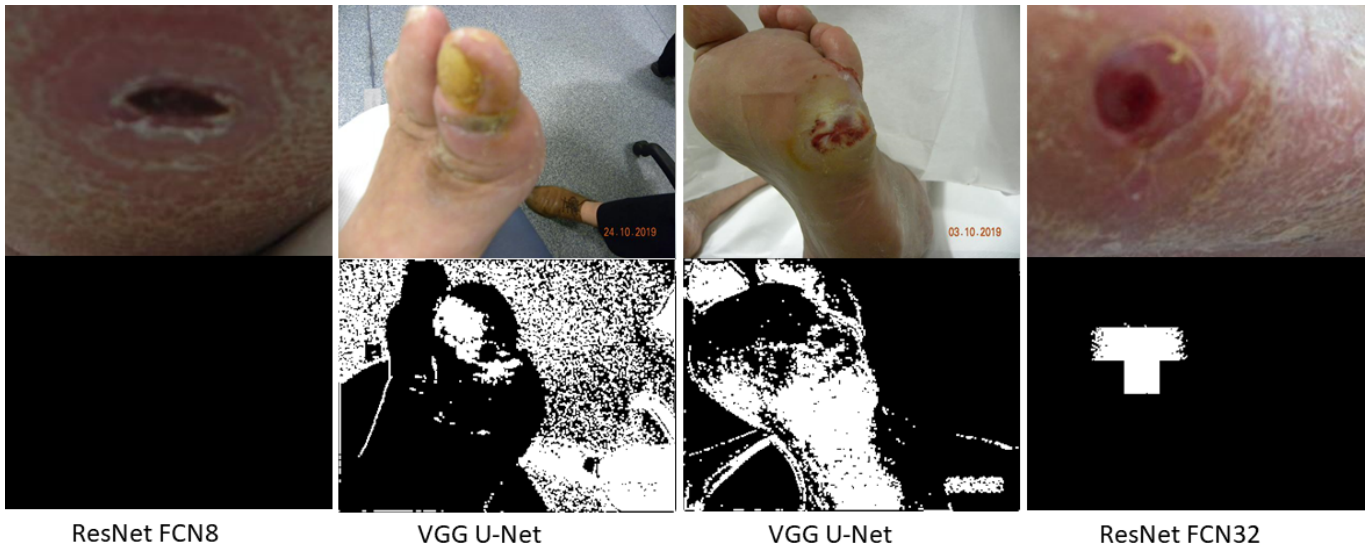


Fig. 3. Illustration of issues associated with the baseline models: (Left) An example over down-sampling removing lesion; (Middle-left) example of background noise effecting prediction; (Middle-right) example of region similarity preventing accurate segmentation; and (Right) example of rapid up-sampling producing a block artefact. Left and right images cropped to DFU region. Note: some images were cropped to focus on DFU region.

background noise and focus on the wounds.

## VI. DISCUSSION

We highlighted that the best performing baseline methods had several difficulties which reduced model performance, as shown in Figure 3:

- *Excessive down-sampling of images*: Many of the segmentation backbones are based on classification networks in which reducing to core features is essential. However, with the small image to ratio size of the wounds, this removes the full wound from the image.
- *Data distribution*: As show in figure 2, a large proportion of the dataset has a DFU to background ratio of <5%.

This represents a large dataset bias towards none-DFU regions. This causes the networks to prioritize on the background class over DFU region, and in some cases the DFU class is ignored.

- *Background noise*: Owing to the shape and location of DFU and patient mobility, many of the images contain a wide assortment of noise. In some cases the foot is surrounded by a blue or white cloth so the network can focus, but in many cases the background contains clothes, floor details and other medical equipment. This poses a difficulty and the network must learn to cope with a large variety of background data.
- *Region similarity*: With many cases of DFU the textural

quality of the lesion is similar to that of the surrounding skin, especially in cases of infection. The textural similarity of DFU regions, periwound and surrounding skin regions, introduces difficulty in distinguish the regions. This means that the networks struggled to differentiate between the DFU and other parts of the foot.

- *Rapid up-sampling*: Due to the focus of the backbones ability to output valid feature maps the head of the network is usually light weight. This results in the up-sampling output being performed at a high rate, causing pixelated regions, in addition to small false detection regions.

These issues are the cause of the difficulties the baseline models produce. Oversampling removes the smaller wounds, which amplifies the problem of data distribution, where most wounds are below 5% of the total image size, meaning the networks focus more on the background than on the DFU regions. Furthermore this focus on the background data is amplified by the inconstant and noisy data. Owing to this, the region similarity of the DFU, periwound and surrounding skin is made difficult causing some networks to focus on the entire foot over the DFU regions, as there is too much focus on background data. Finally, the networks perform well using the smoothed masks over the original jagged contours provided by clinicians. Thus, in the final stages when re-upsampling to the desired size, pixelation occurs due to the rapid up-sampling, producing block-like segmentation that requires additional post-processing to smooth and remove small regions.

## VII. CONCLUSION

In this paper we introduce the largest available DFU dataset containing 2000 annotated training images and 2000 test images without annotations, together with the capability of online evaluation of network predictions. We also provide challenging cases, such as none-DFU cases and images resulting from annotator disagreement. We then provide a series of baselines on state-of-the-art models with explainable AI techniques.

We demonstrate that by performing preprocessing on the expert delineation to smooth the DFU regions, the networks were able to produce more accurate DFU segmentation results. This was shown by comparing a cross validation between raw and smoothed masks. From this study we perform an ablation study on widely used semantic segmentation networks, producing a set of baseline results. The prediction results from the trained models highlights the difficulty in DFU clinical delineation where inter reliability can be inconsistent. This work sheds light on the challenges inherent in the development of AI systems which can aid the standardisation of DFU delineation over time to track healing progress.

## REFERENCES

- [1] E. Ghanassia, L. Villon, J.-F. dit Dieudonne, C. Boegner, A. Avignon, and A. Sultan, "Long-term outcome and disability of diabetic patients hospitalized for diabetic foot ulcers: a 6.5-year follow-up study," *Diabetes care*, vol. 31, no. 7, pp. 1288–1292, 2008.
- [2] W. J. Jeffcoate and K. G. Harding, "Diabetic foot ulcers," *The lancet*, vol. 361, no. 9368, pp. 1545–1551, 2003.
- [3] P. R. Cavanagh, B. A. Lipsky, A. W. Bradbury, and G. Botek, "Treatment for diabetic foot ulcers," *The Lancet*, vol. 366, no. 9498, pp. 1725–1735, 2005.
- [4] K. Ogurtsova, S. Morbach, B. Haastert, M. Dubský, G. Rümenapf, D. Ziegler, A. Jirkovska, and A. Icks, "Cumulative long-term recurrence of diabetic foot ulcers in two cohorts from centres in Germany and the Czech Republic," *Diabetes research and clinical practice*, vol. 172, p. 108621, 2021.
- [5] A. Ahmad, M. Abujbara, H. Jaddou, N. A. Younes, and K. Ajlouni, "Anxiety and depression among adult patients with diabetic foot: prevalence and associated factors," *Journal of clinical medicine research*, vol. 10, no. 5, p. 411, 2018.
- [6] F. M. Davis, A. Kimball, A. Boniakowski, K. Gallagher, and K. Gallagher, "Dysfunctional Wound Healing in Diabetic Foot Ulcers : New Crossroads," 2018.
- [7] M. Edmonds, C. Manu, and P. Vas, "The current burden of diabetic foot disease," *Journal of Clinical Orthopaedics and Trauma*, vol. 17, pp. 88–93, 2021.
- [8] R. Sorber and C. J. Abularrage, "Diabetic foot ulcers: Epidemiology and the role of multidisciplinary care teams," in *Seminars in vascular surgery*, vol. 34, no. 1. Elsevier, 2021, pp. 47–53.
- [9] M. Chang and T. T. Nguyen, "Strategy for treatment of infected diabetic foot ulcers," *Accounts of chemical research*, vol. 54, no. 5, pp. 1080–1093, 2021.
- [10] K. Glover, A. C. Stratakos, A. Varadi, and D. A. Lamprou, "3D scaffolds in the treatment of diabetic foot ulcers: new trends vs conventional approaches," *International Journal of Pharmaceutics*, vol. 599, p. 120423, 2021.
- [11] Z. J. Lo, N. K. Surendra, A. Saxena, and J. Car, "Clinical and economic burden of diabetic foot ulcers: A 5-year longitudinal multi-ethnic cohort study from the tropics," *International Wound Journal*, vol. 18, no. 3, pp. 375–386, 2021.
- [12] H. Sun, P. Saeedi, S. Karuranga, M. Pinkepank, K. Ogurtsova, B. B. Duncan, C. Stein, A. Basit, J. C. N. Chan, J. C. Mbanya, and Others, "IDF diabetes atlas: Global, regional and country-level diabetes prevalence estimates for 2021 and projections for 2045," *Diabetes research and clinical practice*, p. 109119, 2021.
- [13] R. Pranata, J. Henrina, W. M. Raffaello, S. Lawrensia, and I. Huang, "Diabetes and COVID-19: the past, the present, and the future," *Metabolism*, vol. 121, p. 154814, 2021.
- [14] B. Cassidy, N. D. Reeves, J. M. Pappachan, N. Ahmad, S. Haycocks, D. Gillespie, and M. H. Yap, "A cloud-based deep learning framework for remote detection of diabetic foot ulcers," *arXiv preprint arXiv:2004.11853*, 2021.
- [15] M. H. Yap, N. Reeves, A. Boulton, S. Rajbhandari, D. Armstrong, A. G. Maiya, B. Najafi, E. Frank, and J. Wu, "Diabetic foot ulcers grand challenge 2022," Mar. 2021. [Online]. Available: <https://doi.org/10.5281/zenodo.4575228>
- [16] C. Wang, D. M. Anisuzzaman, V. Williamson, M. K. Dhar, B. Rostami, J. Niezgoda, S. Gopalakrishnan, and Z. Yu, "Fully automatic wound segmentation with deep convolutional neural networks," *Scientific Reports*, vol. 10, no. 1, pp. 1–9, 2020. [Online]. Available: <https://doi.org/10.1038/s41598-020-78799-w>
- [17] S. Thomas, "Medetec," 2020, last access: 08/11/21. [Online]. Available: <http://www.medetec.co.uk/index.html>
- [18] C. Wang, B. Rostami, J. Niezgoda, S. Gopalakrishnan, and Z. Yu, "Foot ulcer segmentation challenge 2021," Mar. 2021. [Online]. Available: <https://doi.org/10.5281/zenodo.4575314>
- [19] B. Cassidy, N. D. Reeves, J. M. Pappachan, D. Gillespie, C. O'Shea, S. Rajbhandari, A. G. Maiya, E. Frank, A. J. M. Boulton, D. G. Armstrong, B. Najafi, J. Wu, R. S. Kochhar, and M. H. Yap, "The dfuc 2020 dataset: Analysis towards diabetic foot ulcer detection," *touchREVIEWS in Endocrinology*, vol. 17, pp. 5–11, 2021. [Online]. Available: <https://www.touchendocrinology.com/diabetes/journal-articles/the-dfuc-2020-dataset-analysis-towards-diabetic-foot-ulcer-detection/1>
- [20] M. H. Yap, B. Cassidy, J. M. Pappachan, C. O'Shea, D. Gillespie, and N. D. Reeves, "Analysis Towards Classification of Infection and Ischaemia of Diabetic Foot Ulcers," in *Proceedings of the IEEE EMBS International Conference on Biomedical and Health Informatics (BHI 2021)*, 2021, pp. 1–4.
- [21] M. H. Yap, C. Kendrick, N. Reeves, M. Goyal, J. Pappachan, and B. Cassidy, *Development of Diabetic Foot Ulcer Datasets: An Overview*, 01 2022, pp. 1–18.
- [22] M. Goyal, M. H. Yap, N. D. Reeves, S. Rajbhandari, and J. Spragg, "Fully convolutional networks for diabetic foot ulcer segmentation," in

- 2017 *IEEE International Conference on Systems, Man, and Cybernetics (SMC)*, Oct 2017, pp. 618–623.
- [23] C. Wang, A. Mahbod, I. Ellinger, A. Galdran, S. Gopalakrishnan, J. Niezgod, and Z. Yu, “Fuseg: The foot ulcer segmentation challenge,” 2022. [Online]. Available: <https://arxiv.org/abs/2201.00414>
- [24] A. Mahbod, R. Ecker, and I. Ellinger, “Automatic foot ulcer segmentation using an ensemble of convolutional neural networks,” 2021. [Online]. Available: <https://arxiv.org/abs/2109.01408>
- [25] D.-J. Kroon, “Snake: Active contour,” Online, Jan. 2022. [Online]. Available: <https://www.mathworks.com/matlabcentral/fileexchange/28149-snake-active-contour>
- [26] M. Goyal and M. H. Yap, “Multi-class semantic segmentation of skin lesions via fully convolutional networks,” *arXiv preprint arXiv:1711.10449*, 2017.
- [27] L.-C. Chen, G. Papandreou, I. Kokkinos, K. Murphy, and A. L. Yuille, “Deeplab: Semantic image segmentation with deep convolutional nets, atrous convolution, and fully connected crfs,” *IEEE transactions on pattern analysis and machine intelligence*, vol. 40, no. 4, pp. 834–848, 2017.
- [28] Z. Khan, N. Yahya, K. Alsaih, S. S. A. Ali, and F. Meriaudeau, “Evaluation of deep neural networks for semantic segmentation of prostate in t2w mri,” *Sensors*, vol. 20, no. 11, 2020. [Online]. Available: <https://www.mdpi.com/1424-8220/20/11/3183>
- [29] R. Azad, M. Asadi-Aghbolaghi, M. Fathy, and S. Escalera, “Attention deeplabv3+: Multi-level context attention mechanism for skin lesion segmentation,” in *Computer Vision – ECCV 2020 Workshops*, A. Bartoli and A. Fusiello, Eds. Cham: Springer International Publishing, 2020, pp. 251–266.
- [30] J. Long, E. Shelhamer, and T. Darrell, “Fully convolutional networks for semantic segmentation,” in *Proceedings of the IEEE Conference on Computer Vision and Pattern Recognition*, 2015, pp. 3431–3440.
- [31] O. Ronneberger, P. Fischer, and T. Brox, “U-net: Convolutional networks for biomedical image segmentation,” in *International Conference on Medical Image Computing and Computer-Assisted Intervention*. Springer, 2015, pp. 234–241.
- [32] V. Badrinarayanan, A. Kendall, and R. Cipolla, “Segnet: A deep convolutional encoder-decoder architecture for image segmentation,” *IEEE transactions on pattern analysis and machine intelligence*, vol. 39, no. 12, pp. 2481–2495, 2017.
- [33] K. Simonyan and A. Zisserman, “Very deep convolutional networks for large-scale image recognition,” *arXiv preprint arXiv:1409.1556*, 2014.
- [34] K. He, X. Zhang, S. Ren, and J. Sun, “Deep residual learning for image recognition,” in *Proceedings of the IEEE conference on computer vision and pattern recognition*, 2016, pp. 770–778.